

Interplanar coupling, induced superconductivity, and van Hove singularity in high- T_c cuprates

J. L. Tallon and G. V. M. Williams

The New Zealand Institute for Industrial Research, P. O. Box 31310, Lower Hutt, New Zealand

C. Bernhard

Fakultät für Physik, Universität Konstanz, D-78434 Konstanz, Germany

D. M. Pooke and M. P. Staines

The New Zealand Institute for Industrial Research, P. O. Box 31310, Lower Hutt, New Zealand

J. D. Johnson

Interdisciplinary Research Centre in Superconductivity, Cambridge University, Cambridge, CB3 0HE, United Kingdom

R. H. Meinhold

The New Zealand Institute for Industrial Research, P. O. Box 31310, Lower Hutt, New Zealand

(Received 11 December 1995)

The interplanar coupling between the superconducting CuO_2 planes in $\text{RBa}_2\text{Cu}_3\text{O}_{7-\delta}$ is controlled by changing the size of the rare earth and by changing the oxygen deficiency in the chains while keeping the hole concentration on the planes fixed at optimum doping by means of Ca substitution on the R site. The irreversibility field $H_{\text{irr}}(T)$, thermopower, penetration depth from muon spin rotation, and the c -axis coherence length from fluctuation conductivity all indicate superconductivity extends onto the $\text{CuO}_{1-\delta}$ chains by the proximity effect, giving an increased interlayer coupling equivalent to a halving of the interplanar distance. The insensitivity of T_c to interlayer coupling and the absence of a peak in the density of states determined from Y NMR seriously erodes the van Hove singularity scenario for the high- T_c cuprates. [S0163-1829(96)51118-5]

The $\text{CuO}_{1-\delta}$ chains in $\text{RBa}_2\text{Cu}_3\text{O}_{7-\delta}$ (123) become metallic when $\delta \rightarrow 0$ and strongly influence the transport, infrared, and superconducting properties.¹ This has largely been overlooked since the discovery of this material and many studies devote little attention to the precise oxygen content of the chains and the accurate doping state of the planes. This is particularly the case for single crystals which are difficult to fully oxygenate and when a T_c value of 90 K is quoted it is not clear whether the sample is slightly underdoped or overdoped. Depending on which is the case the condensate density, condensation energy, irreversibility field, and critical current density each may take widely different values, the first two due to additional contributions arising from the order parameter extending onto the chains, and the second two due to the additional interlayer coupling mediated by the chains.

We have sought to separate the plane and chain contributions to physical properties by investigating a variety of 123 compounds with different degrees of oxygenation but having the same optimal hole concentration in the planes so that T_c has the value $T_{c,\text{max}}$ at the peak of the roughly parabolic superconducting phase curve.² In Ca-substituted 123 substantial overdoping can be achieved and, by depleting oxygen, the compound may be brought back to optimal doping. We have used the thermopower to determine the doping state³ and to accurately achieve optimal doping. In such optimal compounds δ_{opt} increases with the mole fraction, x , of calcium and thus the effects of oxygen disorder on the chains can be investigated while the doping state of the planes remains unchanged. In addition, the *interpair* interplanar cou-

pling can thus be continuously varied. Bromine exchange on the chains also allows optimal doping on the planes while destroying the metallicity of the chains.¹ Finally, by changing the size of the rare-earth ion the charge distribution between chains and planes is altered such that the optimal oxygen deficiency decreases with increasing rare-earth size and is close to zero (≈ 0.02) for $R=\text{Nd}$.⁴ The size of the rare-earth ion also determines the degree of *intrapair* interplanar coupling. Using such optimized materials we have already presented evidence from muon spin relaxation (μSR) for proximity-induced superconductivity on fully oxygenated chains.¹ The inset to Fig. 1 shows the low-temperature μSR depolarization rate, $\sigma_0 \sim n_s/m^*$, for optimized samples plotted as a function of δ as reported in Ref. 1. This reveals a strongly enhanced condensate density, n_s , at low δ due to pair condensation of the chain carriers. As the metallicity and superconductivity of the chains is destroyed with increasing δ , n_s is seen to reduce to a value arising just from the planes and typical of other chain-free optimal cuprates such as $\text{Bi}_2\text{Sr}_2\text{CaCu}_2\text{O}_{8+\delta}$. In the following we present further evidence for proximity-induced chain superconductivity and a resulting strongly enhanced interplanar coupling and irreversibility field, H_{irr} .

A second issue to emerge from the present studies is the implication of the observed dependence of T_c on interplanar coupling for the van Hove singularity (vHS) scenario. The vHS corresponds to a saddle point in the quasi-two-dimensional band-structure energy-surface resulting in a logarithmic singularity in the density of states (DOS).⁵ The strongly enhanced DOS presents the twin merits of the pos-

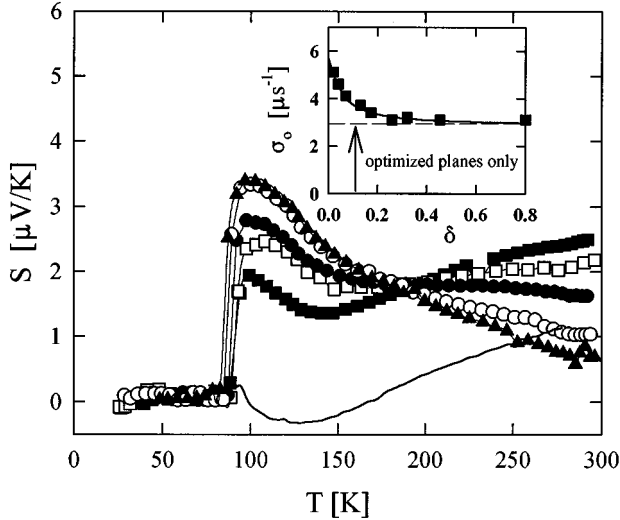


FIG. 1. The temperature dependence of the thermoelectric power, $S(T)$, for optimally doped $\text{EuBa}_2\text{Cu}_3\text{O}_{6.97}$ (solid curve) and optimally doped $\text{Y}_{1-x}\text{Ca}_x\text{Ba}_2\text{Cu}_3\text{O}_{7-\delta}$ (■: $x=0$, $\delta=0.12$; □: $x=0.05$, $\delta=0.19$; ●: $x=0.10$, $\delta=0.25$; ○: $x=0.15$, $\delta=0.31$; ▲: $x=0.20$, $\delta=0.40$). Inset: the variation in μSR depolarization rate with oxygen deficiency in optimally doped $\text{Y}_{1-x}\text{Ca}_x\text{Ba}_2\text{Cu}_3\text{O}_{7-\delta}$ showing the underlying contribution from the planes and the excess contribution from the chains.

sibility of a high T_c and the occurrence of an optimal maximum in T_c as the vHS sweeps through the Fermi energy with increasing carrier doping. It potentially accounts, therefore, for the paraboliclike dependence of T_c on hole concentration, p . Within this model the thermoelectric power is expected to change both sign and slope at optimal doping and the approximate occurrence of this behavior for $\text{YBa}_2\text{Cu}_3\text{O}_{7-\delta}$ has been presented as evidence for the vHS model.⁶ The logarithmic singularity in the DOS occurs only for the truly two-dimensional (2D) system and, with increasing three-dimensionality arising from interplanar coupling, the peak in the DOS should broaden out and T_c decrease due to the reduced DOS. These ideas are readily investigated in the presently described materials and we find they are not sustained.

Polycrystalline samples of $\text{Y}_{1-x}\text{Ca}_x\text{Ba}_2\text{Cu}_3\text{O}_{7-\delta}$ with $x=0, 0.05, 0.10, 0.15$, and 0.2 were made by standard solid-state reaction methods using high-purity powders, except that the reaction was started at 910°C in air, then stepwise increased (with intermediate grindings) by 10 up to 970°C and finally sintered at 1000°C in oxygen. The incrementally high temperatures for synthesis is necessary to suppress partial substitution of Ca for Ba.^{1,2} Oxygen loading is carried out by slow cooling in oxygen to as low as 320°C , as is necessary to achieve maximal loading and hence maximal overdoping. For $x=0.2$ overdoped T_c values as low as 47 K can be achieved.

For each of the other rare-earth 123 systems different oxygen partial pressures were required to produce single-phase 123 material: oxygen at 940°C for Yb, air at 940°C for $R=\text{Er, Dy, Y, Gd}$, and Eu and an oxygen partial pressure of 100 Pa at 865°C for Nd. Preliminary reactions were carried out at lower temperatures which were incremented with intermediate grindings. Brominated samples of

$\text{YBa}_2\text{Cu}_3\text{O}_{7-\delta}$ were prepared by unloading oxygen from a polycrystalline sample to $\delta\approx 0.8$ which was then sealed in a quartz tube with liquid bromine at the other end and warmed to 260°C where it was kept for 20 min . This resulted in a rapid uptake of bromine and transformation of the insulating 123 material to a 92 K superconductor. Oxygen deficiencies, δ , were determined from mass changes relative to maximum loading for which the oxygen content was determined by neutron diffraction refinements.² Thermoelectric power measurements were made using conventional techniques with Pb as a reference standard. The fluctuation conductivity was determined using four-terminal resistivity measurements by subtracting out the extrapolated normal-state conductivity obtained from a linear- T fit to the resistivity from 150 to 300 K . Irreversibility lines, $H_{\text{irr}}(T)$, were determined using a vibrating-sample magnetometer by plotting ΔM vs field and ascertaining the field, H_{irr} , at which ΔM fell below the threshold criterion 10^{-4} emu/cm^3 . Room-temperature $^{89}\text{Y-NMR}$ shifts were measured on powder samples using a Unity-500 spectrometer with a magic angle spinning (MAS) probe and referenced to YCl_3 .

Figure 1 shows $S(T)$ for $\text{EuBa}_2\text{Cu}_3\text{O}_{6.97}$ (solid curve) and $\text{Y}_{1-x}\text{Ca}_x\text{Ba}_2\text{Cu}_3\text{O}_{7-\delta}$ with $x=0, 0.05, 0.10, 0.15$, and 0.2 with each optimized at $T_c=T_{c,\text{max}}$. The optimized δ values are, respectively, $0.03, 0.12, 0.19, 0.25, 0.31$, and 0.40 . [The $\text{EuBa}_2\text{Cu}_3\text{O}_{7-\delta}$ is slightly overdoped as can be seen by the lower absolute value of $S(T)$.] These samples, which each have the same doping state in the planes, have progressively reduced metallicity in the chains resulting in a gradual shift in $S(T)$ from a positive slope (arising from the chains) to the negative slope characteristic of all other high-temperature superconductor (HTS) cuprates which lack CuO chains. This progression can be seen in unsubstituted $\text{YBa}_2\text{Cu}_3\text{O}_{7-\delta}$ just with increasing δ values³ but because p for this compound is progressively decreased with increasing δ the curves move steadily upwards. As $\text{YBa}_2\text{Cu}_3\text{O}_{7-\delta}$ is significantly overdoped when $\delta\approx 0$ this results in a set of curves which appear to reflect about the x axis. This has been taken as evidence for a vHS sweeping through the Fermi energy at optimum doping⁶ but in Fig. 1 the reversal of slope for the Ca-substituted samples can be seen to originate solely from the destruction of the chain contribution as the doping state of the planes remains fixed. Elsewhere we show that the slope reversal can be displaced arbitrarily far into the overdoped region by Ca substitution and is thus unrelated to the vHS scenario.⁷ Figure 1 confirms a set of samples in which the chain contribution to transport and interplanar coupling is progressively destroyed.

The inset to Fig. 2 shows the square of the measured fluctuation resistivity (data points) plotted as a function of temperature for optimally doped $R\text{Ba}_2\text{Cu}_3\text{O}_{7-\delta}$ with $R=\text{Eu, Gd, Y, and Yb}$. Within the Lawrence-Doniach model⁸ of stacked two-dimensional sheets the fluctuation conductivity, $\Delta\kappa$, is

$$\Delta\kappa = \pi e^2 \{ 16\hbar d_i \epsilon [1 + (2\xi_c/d_i)^2 (1/\epsilon)]^{1/2} \}^{-1}, \quad (1)$$

where $\epsilon = (T - T_c)/T_c$, ξ_c is the c -axis coherence length at $T=0\text{ K}$ and d_i is the interlayer spacing between superconducting sheets, usually the ‘‘plane-to-plane’’ distance between CuO_2 sheets. The solid curves in the inset to Fig. 2 are fits of Eq. (1) to the experimental data using ξ_c/d_i as the

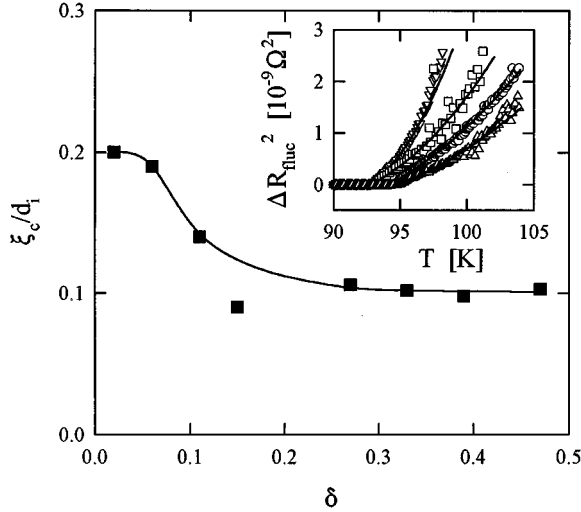


FIG. 2. The variation in c -axis coherence length with oxygen deficiency for optimally doped $R\text{Ba}_2\text{Cu}_3\text{O}_{7-\delta}$ (with $R=\text{Eu, Gd, Y, and Yb}$) and $\text{Y}_{1-x}\text{Ca}_x\text{Ba}_2\text{Cu}_3\text{O}_{7-\delta}$. Inset: the temperature dependence of the square of the fluctuation resistance.

fitting parameter. The values of ξ_c/d_i thus determined are plotted in Fig. 2 versus the δ value for each optimized compound we have investigated, including the $\text{Y}_{1-x}\text{Ca}_x\text{Ba}_2\text{Cu}_3\text{O}_{7-\delta}$ samples. Apart from the unsystematically low data point for Yb-123, which compound is unusual in several properties, the ratio appears to double its value from ≈ 0.1 at high oxygen deficiency to ≈ 0.2 as $\delta \rightarrow 0$. Because the doping state is the same for each of these compounds it is reasonable to assume the same constant value for ξ_c and interpret these results in terms of a progressive halving of the effective value of d_i from the *plane-to-plane* distance when $\delta > 0.3$ (and only the CuO_2 planes superconduct) to the *plane-to-chain* distance when $\delta \rightarrow 0$ (and the chain layer also superconducts by proximity effect).

We have previously determined the irreversibility field, $H_{\text{irr}}(T)$, for several optimally doped polycrystalline HTS cuprates additional to the rare-earth and Ca-doped 123 systems noted above and found that the complete data set for these compounds can be scaled to a single curve, $H^*(T/T_{c,\text{max}})$ and the scaling parameter, consistent with a c -axis tunnelling picture, varies exponentially with d_i .⁹ H_{irr} at $T=0.75T_c$ is plotted versus d_i in Fig. 3. The data plotted for Y-123 is for fully oxygen-loaded material with $\delta \approx 0.03$. Significantly, if the true interplanar distance of 8.4 \AA is chosen for Y-123, H_{irr} shown by the open symbol is too high and does not fit the exponential correlation satisfied by the Bi-, Tl-, and Hg-cuprates. If, however, due to proximity-induced superconductivity on the fully oxygenated chains the relevant coupling distance is chosen to be the plane-to-chain distance of 4.2 \AA then the data point, shown by the solid symbol, fits the correlation well. This appears to be also satisfied by the fully oxygenated 247 material which, like 123, has strong flux pinning and a high irreversibility field¹⁰ due to induced chain superconductivity.¹ For both 123 and 247 it is implicit that the shortening of the effective coupling distance results in an eight-fold increase in irreversibility field. This was checked by determining $H_{\text{irr}}(T)$ for *optimally doped* $\text{Y}_{0.8}\text{Ca}_{0.2}\text{Ba}_2\text{Cu}_3\text{O}_{6.60}$ and the brominated $\text{YBa}_2\text{Cu}_3\text{O}_{6.2}$ sample. Both of these have inactive chain layers and indeed

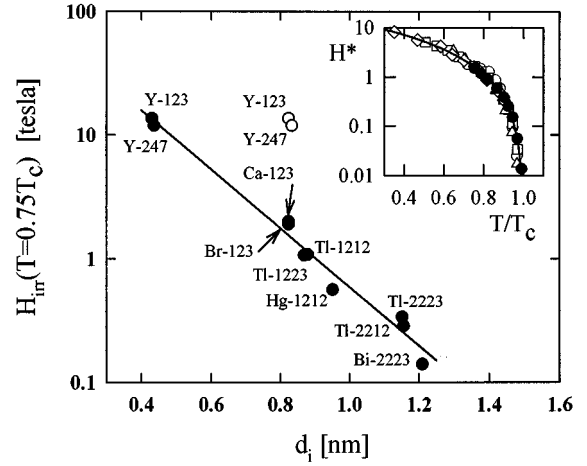


FIG. 3. The dependence of the irreversibility field, H_{irr} at $0.75 T_c$ on the blocking layer distance, d_i . The open data points for Y-123 and Y-247 are for $d_i = \text{“plane-to-plane”}$ distance and the solid data points for Y-123 and Y-247 are for $d_i = \text{“plane-to-chain”}$ distance. Inset: the irreversibility field for optimally doped $\text{Y}_{1-x}\text{Ca}_x\text{Ba}_2\text{Cu}_3\text{O}_{7-\delta}$ scaled, by a multiplicative constant, to a single curve. \circ : $x=0.0$, $\delta=0.12$; \square : $x=0.05$, $\delta=0.19$; ∇ : $x=0.10$, $\delta=0.25$; \triangle : $x=0.15$, $\delta=0.31$; \diamond : $x=0.20$, $\delta=0.40$. \bullet : fully oxygen-loaded $\text{YBa}_2\text{Cu}_3\text{O}_{6.97}$.

we find the data points, denoted in Fig. 4 by “Ca-123” and “Br-123” respectively, are consistent with the coupling length having now doubled to equal the plane-to-plane distance consistent with the suppression of chain superconductivity. Thus both the fluctuation conductivity and irreversibility field data independently support a picture where the effective coupling distance is halved due to the superconducting order parameter extending onto the chains by proximity effect.

The remarkable feature of the above results is that, despite the considerable changes in interplanar coupling achieved by altering the size of the rare-earth element or by changing the oxygen deficiency while keeping optimum doping on the planes, there is little change in T_c . We have already drawn attention to the complete independence of $T_{c,\text{max}}$ on interpla-

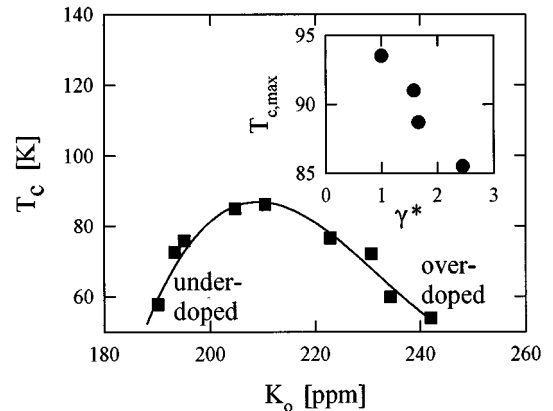


FIG. 4. The variation of T_c and Knight shift parameter, K_0 (proportional to the DOS) for $\text{Y}_{0.8}\text{Ca}_{0.2}\text{Ba}_2\text{Cu}_3\text{O}_{7-\delta}$ for different values of δ extending from the heavily underdoped to heavily overdoped regions. Inset: the variation of $T_{c,\text{max}}$ with anisotropy, $\gamma^* = \gamma/\gamma_0$, for optimally doped $\text{Y}_{1-x}\text{Ca}_x\text{Ba}_2\text{Cu}_3\text{O}_{7-\delta}$.

nar coupling in the 123 system $\text{Yb}_{1-x}\text{Ca}_x\text{Ba}_{1.6}\text{Sr}_{0.4}\text{Cu}_3\text{O}_{7-\delta}$ which remains at 82 K irrespective of the value of x .⁹ We illustrate this for the presently investigated materials as follows. The irreversibility lines which we have measured for the *optimized* $\text{Y}_{1-x}\text{Ca}_x\text{Ba}_2\text{Cu}_3\text{O}_{7-\delta}$ materials steepen markedly with reduction in δ and scale onto a single curve, $H^*(T)$, which is shown in the inset to Fig. 3. This curve is, in fact, the data set for $x=0.2$ ($\delta=0.40$) with the remaining $H_{\text{irr}}(T/T_c)$ curves for smaller values of x scaled onto this line, the scaling factor decreasing sharply with increasing δ and, hence, increasing anisotropy. We estimate the anisotropy $\gamma = \lambda_c / \lambda_{ab}$, where λ is the London penetration depth, directly from the square root of the scaling factors for $H^*(T)$. The motivation for this is that Hardy *et al.*¹¹ have pointed out that several models for the irreversibility line (including flux-lattice melting and Josephson decoupling) all have $H_{\text{irr}}(T) \propto \gamma^{-2}$. We note that all other parameters contributing to $H_{\text{irr}}(T)$ for a set of samples each at optimum doping do not vary because of the fixed doping state of the planes. As a consequence the scaling factors vary as γ^{-2} . The optimized $T_{c,\text{max}}$ values are plotted in the inset to Fig. 4 as a function of γ^* ($= \gamma/\gamma_0$, the anisotropy ratioed to that at $x=0$). The steadily decreasing values of T_c with increasing anisotropy seriously prejudice the vHS scenario which implicates the reverse situation: T_c should decrease with decreasing anisotropy as the peak in the DOS broadens out due to interplanar coupling.

Finally, we wish to point out from our Y-NMR investigations that there is in fact no evidence for a peak in the DOS as a function of hole concentration. We have determined the room-temperature Y-NMR Knight shifts for $\text{Y}_{0.8}\text{Ca}_{0.2}\text{Ba}_2\text{Cu}_3\text{O}_{7-\delta}$ for a range of δ values extending from the heavily overdoped region ($T_c=49$ K), through optimum doping ($T_{c,\text{max}}=85.5$ K) to the underdoped region ($T_c=70$ K). Hole concentrations, p , were estimated using the room-temperature thermoelectric power and the previously reported correlation³ with p . The Knight shift in the underdoped and slightly overdoped regimes has been shown to be well described by¹²

$$K(T) = K_0 \operatorname{sech}^2(E_g/2kT) + \sigma, \quad (2)$$

where σ is the temperature-independent chemical shift (152 ppm) and the temperature-dependent term describes the effect of the normal-state gap with gap energy E_g . The prefactor K_0 contains the Pauli susceptibility and is thus proportional to the DOS at the Fermi level. The p dependence of E_g has been determined previously from the temperature dependence of the Y-NMR Knight shifts for 123, 247, and 124 at various hole concentrations¹³ as well as from Gd-esr Knight shifts.¹² Taking these E_g values we have used Eq. (2) to determine K_0 for our $\text{Y}_{0.8}\text{Ca}_{0.2}\text{Ba}_2\text{Cu}_3\text{O}_{7-\delta}$ samples from the room-temperature Knight shift. The T_c values are plotted as a function of K_0 in Fig. 4. While T_c rises then falls with doping the DOS, represented by K_0 is a smooth, monotonically increasing function of hole doping and there is no suggestion of a peak in K_0 at, or near, optimum doping where T_c maximizes. In the vHS scenario the curve in Fig. 4 would follow a reflex loop with positive slope in both the under- and overdoped regions. Our results are confirmed by high-precision measurements of $\gamma^{\text{el}} = dC_p^{\text{el}}/dT$.¹⁴ Well above T_c γ^{el} , like K_0 , is featureless and does not peak at optimum doping. We conclude that the vHS scenario is unsupported by the doping dependence of the thermoelectric power (TEP), the dependence of $T_{c,\text{max}}$ on interlayer coupling, and the doping dependence of the density of states. Even if, as in some models,¹⁵ the vHS is pinned close to the Fermi energy and does not sweep past E_F with doping the relative independence (and indeed, reverse dependence) of T_c on interlayer coupling is inconsistent with the vHS model.

In summary, we have investigated a set of 123 compounds in which the CuO_2 planes are kept at optimum doping while the interplanar coupling is varied. The progressive destruction of CuO chain metallicity, chain superconductivity, and interlayer coupling is compellingly revealed by the thermoelectric power, μSR depolarization rate, fluctuation conductivity, and irreversibility field. We present evidence from the last two properties for a doubling of the effective interlayer coupling distance when the chain metallicity is destroyed and show that the doping dependence of the TEP and of the density of states, as well as the anisotropy dependence of $T_{c,\text{max}}$ are all inconsistent with the vHS scenario.

¹J. L. Tallon *et al.*, Phys. Rev. Lett. **74**, 1008 (1995).

²J. L. Tallon *et al.*, Phys. Rev. B **51**, 12 911 (1995).

³S. D. Obertelli, J. R. Cooper, and J. L. Tallon, Phys. Rev. B **46**, 14 928 (1992).

⁴G. V. M. Williams and J. L. Tallon, Physica C **258**, 41 (1996).

⁵C. C. Tsuei *et al.*, Phys. Rev. Lett. **65**, 2724 (1990).

⁶D. M. Newns *et al.*, Phys. Rev. Lett. **73**, 1695 (1994).

⁷J. L. Tallon and C. Bernhard, Phys. Rev. Lett. **75**, 4552 (1995).

⁸W. E. Lawrence and S. Doniach, in *Proceedings of the 12th International Conference on Low Temperature Physics*, Kyoto, Ja-

pan, 1970, edited by E. Kandi (Keiyakol, Tokyo, 1970), p. 361.

⁹J. L. Tallon, in *Critical Currents in Superconductors*, edited by H. W. Weber (World Scientific, Singapore, 1994), Vol. VII, p. 52.

¹⁰M. P. Staines *et al.* (unpublished).

¹¹V. Hardy *et al.*, Physica C **232**, 347 (1994).

¹²G. V. M. Williams *et al.*, Phys. Rev. B **51**, 16 503 (1995).

¹³J. L. Tallon *et al.*, Physica C **235-240**, 1821 (1994).

¹⁴J. W. Loram *et al.*, Phys. Rev. Lett. **71**, 1740 (1993).

¹⁵R. P. Markiewicz, Phys. Rev. Lett. **73**, 1310 (1994).